

Appendix 1

Individual states

C4s, C5s, and adult females are characterised by three state variables: structure x ($\mu\text{g C}$), store y ($\mu\text{g C}$), and habitat z . There are two habitats, $z = \text{surface (active)}$ and $z = \text{deep (diapause)}$.

Structure consists of the exoskeleton, vital organs, and other parts necessary for a functioning copepod.

Structure is 15–120 $\mu\text{g C}$ (106 discrete states, 1 $\mu\text{g C}$ intervals, Fig. 2 main text), cannot decrease, and moulting to the next stage is assumed at fixed structure: 15, 50 and 120 $\mu\text{g C}$ to C4, C5, and adult female, respectively (Fig. 2 main text). Moulting thresholds are based on the lower range of carbon masses of newly moulted C4s and C5s (Shreeve and Ward 1998, Shreeve 2002). Newly moulted adult females have not been measured. Instead, structure was set such that total body mass for adult females with full stores are in the upper range of that observed (Shreeve and Ward 1998, Shreeve et al. 2002).

Store is dynamic and represents body condition. Lipid stores (mainly the oil sac) may constitute up to 50% of individual dry mass (Hagen and Schnack-Schiel 1996). However, proteins must also be present because lipids alone can not fuel structural growth and egg production. In the carbon units used here, we assume that maximum store is three times structure (Fig. 2 main text). Store y is modelled as a percentage (101 discrete states, 1% intervals) of maximum store.

Food availability – Chla

Data from the Scotia Sea are used to parameterize food availability and temperature (Fig. A1, 3a–b). We used satellite-measured (SeaWiFS) chlorophyll a (Chla) levels as a proxy for the seasonality of the food source (Fig. A1). Onset and duration of the phytoplankton bloom vary between years. Some years have a late bloom, others have an early bloom, and a few years seem to have two blooms. Winter conditions always prevail from April to September. SeaWiFS data suggest low Chla concentrations (Fig. A1), and the model predicts poor growth and fecundity using these values. However, *C. acutus* grow well in the Scotia Sea and complete the life cycle in one year (Atkinson et al. 1997, Tarling et al. 2004). This may suggest unrealistic model assumptions or parameterisation. Using surface Chla values, as measured by SeaWiFS may however under-represent experienced food concentrations for at least two reasons. (1) SeaWiFS measurements are lower than in situ measurements at concentrations above 0.2 $\mu\text{g Chla l}^{-1}$, and particularly for values above 1.0 $\mu\text{g Chla l}^{-1}$ (Holm-Hansen et al. 2004). (2) *C. acutus* may not only depend on phytoplankton for food. Through suspension feeding, other food objects are also likely although *C. acutus* is one of the Southern Ocean copepods most closely relying on phytoplankton (Michels and Schnack-Schiel 2005). Maximum food availability is therefore set higher than indicated by SeaWiFS values alone (Fig. 3 main text), and to a level (maximum of 2.0 $\mu\text{g Chla l}^{-1}$) where population growth rate $\lambda \approx 1$ (1.08, 0.67, and 0.99 for the early, intermediate, and late feeding seasons, respectively). Such Chla values are observed in the area (Holm-Hansen et al. 2004).

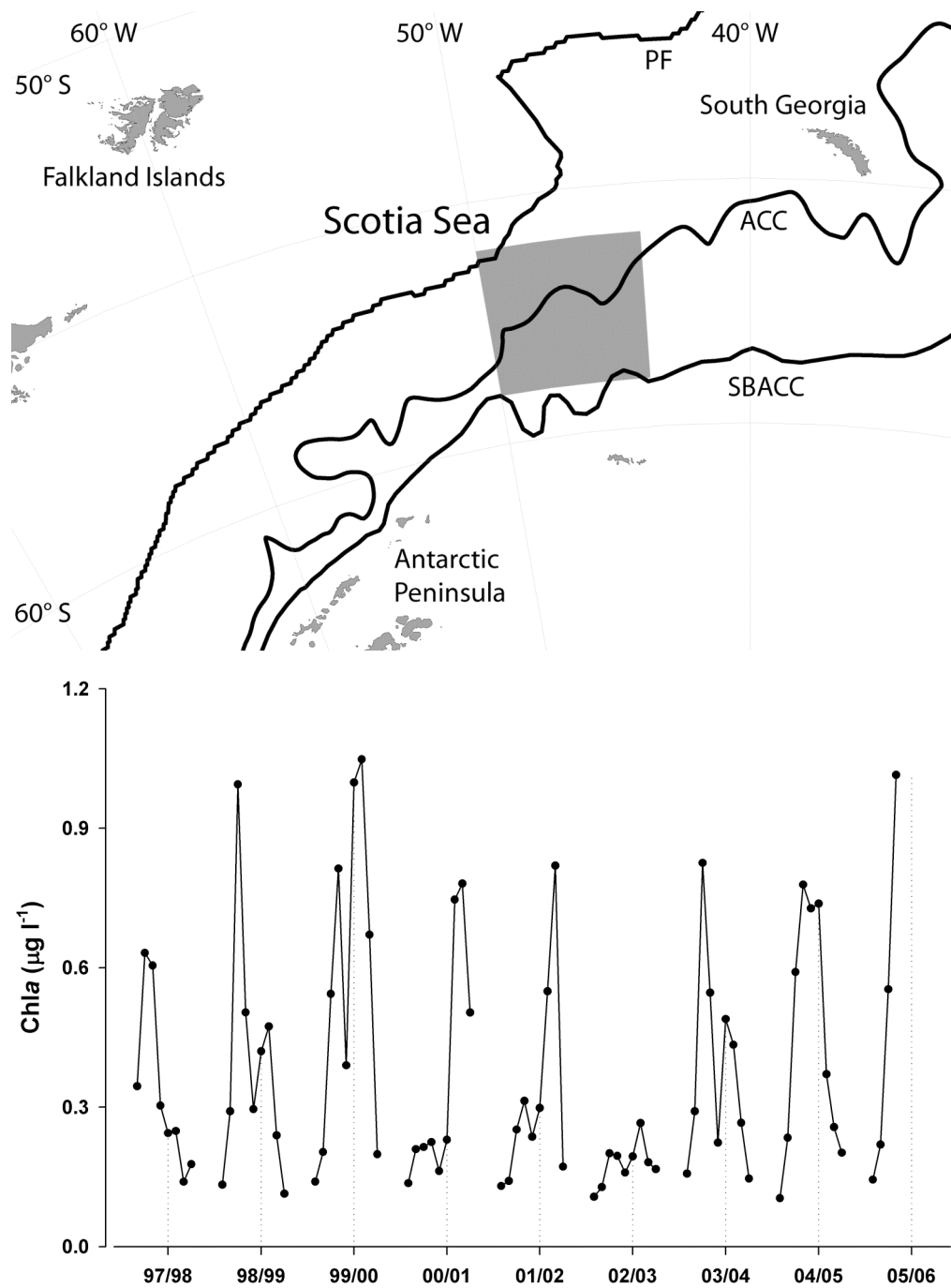


Fig. A1. Upper panel: reference area for environmental forcing in a *Calanoides acutus* life history model. Data on temperature and Chla are from a selected Scotia Sea reference area (59–56°S, 50–44°W, grey box). Advection rates are high and it is unlikely that a life-cycle is completed within the reference area, but we assume the conditions to be typical for *C. acutus*. Some major currents and fronts are indicated; the Antarctic circumpolar current (ACC), the Polar front (PF) and the southern ACC boundary (SBACC), positioned as by Thorpe et al. (2004). Lower panel: monthly averages of surface Chla based on SeaWiFS (satellite) measurements. Data are missing in winter (May, June and July). Drop lines are January values. Data are from GES-DISC Interactive Online Visualization ANd aNalysis Infrastructure (Giovanni) (<http://reason.gsfc.nasa.gov/OPS>).

Growth and metabolism

We let assimilated carbon depend on food availability using a curvilinear saturation function (Fig. A2a). This is inspired by estimates of specific growth rates against Chla measurements (Fig 6.3 in Shreeve 2002), obtained from an area providing food-saturated conditions, $\sim 3\text{--}4 \mu\text{g Chla l}^{-1}$ (Atkinson et al. 1996, Shreeve 2002). We assume that maximum assimilated carbon is the sum of maximum growth g_{max} and routine surface metabolism $r_{\text{surf}}(T)$ (Table A1 for these and other parameters). Specific rate of net carbon gain G_{net} is then the difference between assimilated and respired carbon after assimilated carbon is adjusted for food availability f (Fiksen and Folkvord 1999):

Table A1. Parameters for a life history model of *Calanoides acutus*.

Parameter	Description	Unit	Value	Reference and comments
k_1	Coefficient determining maximum amount of stores used per day ^a	–	0.15	Proportion of structure x
c_{eff}	Conversion efficiency from store to egg and from store to structure	–	0.8	(Saito and Tsuda 2000)
c_{mig}	Migration cost from surface to deep habitat	–	0.2	Proportion of carbon mass (structure x + store y)
E	Carbon mass of egg	$\mu\text{g C}$	0.5	^b
m_{starv}	Seasonally constant starvation rate if y = 0	day^{-1}	1.0	
β	Shape of carbon gain vs. Chla (stage $\geq C4$)	$l (\mu\text{g Chla})^{-1}$	0.7	(Fig. 6.3 in Shreeve 2002)
g_{max}	Maximum carbon growth rate	$\text{g g}^{-1}\text{day}^{-1}$	0.25	When food is unlimited (upper range, fig. 6.3 in Shreeve 2002)
r_{surf}	Metabolic rate in surface habitat	$\text{g g}^{-1}\text{day}^{-1}$	0.05	(Tarling et al. 2004) ^c , ten times higher than r_{deep} (Pasternak et al. 1994)
r_{deep}	Metabolic rate in deep habitat ^d	$\text{g g}^{-1}\text{day}^{-1}$	0.005	(Tarling, et al. 2004) ^c
Q10	Q10 for g_{max} and r_{surf}	–	2.5	Reference temperature 2°C (Shreeve 2002)

(a) The limit is set for the use of store to build structure or produce eggs. Additional stores can be used for routine metabolism and migration costs.

(b) Based on average egg diameter (Ward and Shreeve 1995) and a general relationship between egg mass and egg diameter in copepods (Huntley and Lopez 1992).

(c) We assume a value twice that used by Tarling et al. (2004) because growth is modelled as a function of structure rather than total body mass.

(d) Temperature at depth is not modelled explicitly and r_{deep} is therefore constant.

$$G_{\text{net}}(f, T) = \begin{cases} [g_{\text{max}}(T) + r_{\text{surf}}(T)] \cdot (1 - e^{-\beta f}) - r_{\text{surf}}(T) & \text{if } z = \text{surface} \\ -r_{\text{deep}} & \text{if } z = \text{deep} \end{cases} \quad (\text{A1})$$

where β is the shape of the carbon gain – Chla relationship (Fig. A2a), T is temperature and z is habitat. Consequently, net gain is negative at low food concentrations (Fig. A2a) and in the deep habitat. Growth and surface metabolism depend on temperature using a Q_{10} relationship (Table A1, Fig. A2a). Daily net gain per individual $G(x, f, T)$ is then

$$G(x, f, T) = x \cdot (e^{G_{\text{net}}(f, T)} - 1) \quad (\text{A2})$$

for simplicity referred to as G in the remaining. Note that specific net gain is independent of body mass, but individual gain is proportional to structural mass and independent of store.

The C4s used to estimate growth rate at different food concentrations had low lipid levels (Fig. 5.5 in Shreeve 2002). The growth rates are therefore a good proxy for growth modelled as a function of structure. We use the same specific net gain G_{net} for C5 and adult females, as observations were lacking for these stages. Such growth rates convert to a seasonal peak in egg production of up to 45 eggs (both sexes) $\text{ind}^{-1} \text{day}^{-1}$, in the upper range of observed egg production rates (Shreeve 2002).

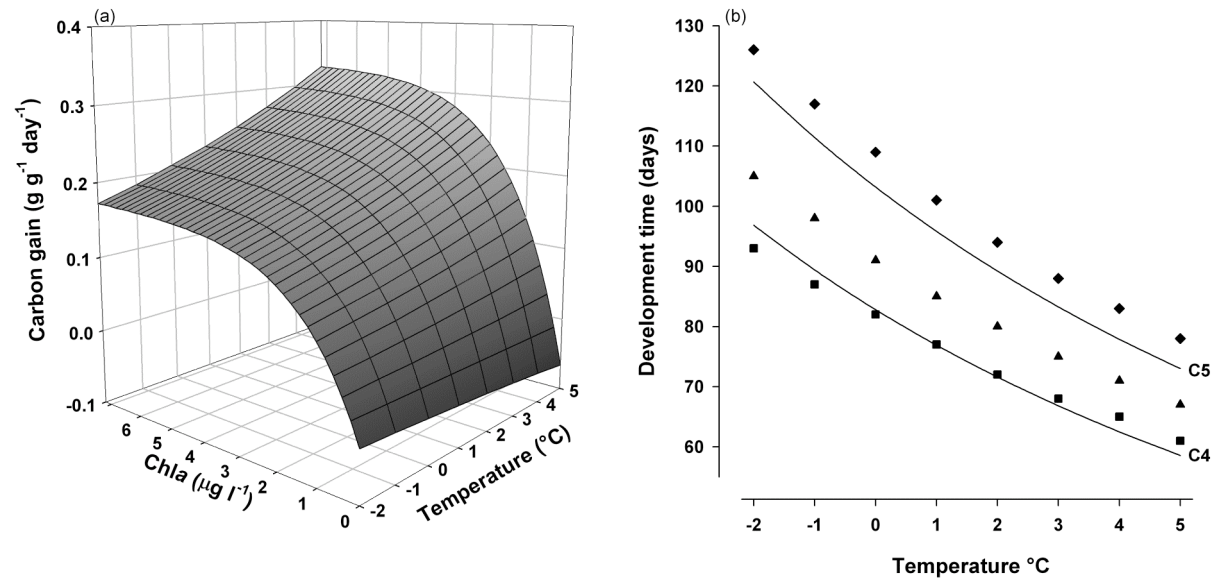


Fig. A2. Growth and development in a life-history model of the copepod *Calanoides acutus*. (a) Modelled net carbon gain vs temperature and food availability of stages C4 to adult female (Eq. A1). Temperature influences net gain via temperature-dependent metabolism and growth. Note that when converting to growth per individual (Eq. A2), the net gain G is a function of structure rather than total body carbon (structure + store). (b) Median development time (MDT) from hatching to stage C4 and C5 at different temperatures. Simulated MDT from the model (symbols) compared with laboratory derived estimates of MDT (lines). The simulated cohort is set to resemble laboratory conditions experiencing non-limited food and the same mortality for all stages. Simulated MDT to C4 is shown with squares. For clarity, C4s and C5s are here given a fixed energy allocation rule α . We present MDT to C5 if 25% (triangles) or 75% is allocated to store (diamonds).

Early development (egg – C3)

A separate submodel for stages prior to C4 closes the life cycle loop and creates explicit links between all stages. Reproductive value of all stages, including the egg, can then be predicted. The purpose of the submodel is to achieve realistic development times from egg to C4. Some observations of early development in *C. acutus* are available, but we also use observations from the similar and well studied *Calanus finmarchicus*.

We make the following assumptions:

- 1) the egg, the six nauplius stages (N1–N6), and the first three copepodite stages (C1–C3) are described by developmental stage rather than structure and store,
- 2) eggs are laid in the surface habitat and remain there until C4 (Atkinson et al. 1997), with development depending on temperature and food availability
- 3) temperature-dependent development follows the shape of the Behlerádek function fitted to observations of hatching time (Ward and Shreeve 1998),
- 4) median development time (MDT, time from laying to 50% of the individuals have reached a certain stage) from egg to C4 is equiproportional to that of *C. finmarchicus* (Campbell et al. 2001) (i.e., the ratio between *C. acutus* and *C. finmarchicus* hatching time and MDT to C4 is the same), and
- 5) each stage from egg to C3 has the same duration when food availability is non-limiting.

Temperature-dependent development time to C4 is then:

$$DT_{\text{temp}}(T) = \left(\frac{a_{10f}}{a_{1f}} \right) \cdot a_{1a} \cdot [T(t) - \alpha_{DT}]^{b_{DT}} \quad (\text{A3})$$

where T is temperature, $a_{10f} = 8798$ and $a_{1f} = 595$ are estimated stage-specific constants for *C. finmarchicus* stage C3 and egg, respectively (Table 3 in Campbell et al. 2001), whereas $a_{1a} = 4883$, $\alpha_{DT} = -27.19$ and $b_{DT} = -2.05$ are constants for a *C. acutus* egg (Ward and Shreeve 1998).

To include food-dependent development, we also assume that:

- 6) N3 is the first stage to feed as for *C. finmarchicus* (Campbell, et al. 2001), and
- 7) development rate is food dependent as for carbon gain of older stages (Eq. A1), but with food limitation at lower Chla concentration, i.e. $\beta_{N3-C3} = 1.0$ (cf. Campbell, et al. 2001).

Expected development time per stage is then:

$$DT(f, T) = \begin{cases} \frac{DT_{\text{temp}}}{\left(1 - e^{-\beta_{N3-C3} \cdot f(t)}\right) \cdot d} & \text{if stage} \geq N3 \\ \frac{DT_{\text{temp}}}{d} & \text{if stage} < N3 \end{cases} \quad (\text{A4})$$

where d is the number of stages and $f (>0)$ is food availability in $\mu\text{g Chla l}^{-1}$. Development rate (reciprocal of development time) is converted to transition probability (moulting probability)

$$P_{\text{trans}}(d, f, T) = 1 - e^{-\left(\frac{1}{DT(f, T)}\right)^{dt \cdot q}} \quad (\text{A5})$$

where dt is time interval (1 day) and q is a constant. In subsequent equations we refer to transition probability by P_{trans} . With daily transition probabilities, there is the rare possibility of spending one day in every stage. To prevent unrealistic numerical diffusion, we assume that all individuals spend at least two days in each developmental stage. An early and late category is introduced for each stage by setting the number of stages $d = 20$ (a stage within stage approach). This causes

longer simulated MDT and we set $q = 1.1$ to achieve the necessary fit with laboratory MDT to C4 (Fig. A2b).

Idealised laboratory conditions were used to compare simulated MDT with laboratory MDT. However, food is limited in the model used to predict optimal life histories, resulting in slower development, in line with observations (Atkinson et al. 1997).

Mortality

Predation rate is higher in the surface habitat (active phase) compared to the deep diapause habitat (Tarling et al. 2004) because of light extinction and higher concentrations of predators such as fish, carnivorous crustaceans, chaetognaths, and seabirds. Additionally, active feeding increases encounter rates with predators compared to the sedate diapause behaviour. Dominant predators as well as seasonal pattern in predation risk are poorly known (Andrews 1966), but we assume a seasonality with peak predation rate at mid-summer (Fig. 3d main text). The seasonality could be driven by light as long days make all visual predators more efficient. Predation rate $m(z,t)$ is assumed independent of structure and store, but empty stores induce a high starvation rate m_{starv} . Tarling et al. (2004) suggested daily mortality (including starvation) of 0.06 day^{-1} during the feeding season, somewhat higher than maximum predation rate used here (Fig. 3d main text). Predation and starvation rates are added and converted to daily survival probability

$P_s(y, z, t) = e^{-\{m(z,t) + m_{\text{starv}}(y)\}}$. For egg to C3 we assume no starvation but a predation rate $m_{\text{egg-C3}}(t)$ higher than for the older stages (Tarling, et al. 2004). Hence, daily survival probability is $P_{\text{sYoung}}(t) = e^{-m_{\text{egg-C3}}(t)}$ (Fig. 3d main text).

Seasonality follows a normal distribution (peak at 1 January, SD = 60 days, Fig. 3d main text). We assume a seasonally constant predation rate in the deep habitat of 0.002 day^{-1} (Fig. 3d main text). Tarling et al. (2004) suggested 0.001 – 0.003 day^{-1} .

Optimised life-history strategies

The modelled copepods (stages C4–adult female) make three life history decisions each day t of the year (Fig. 1 main text):

- (1) Allocation to store or structure (only C4–C5). C4s and C5s allocate carbon between store (a proportion α , between 0 and 1 in steps of 0.1) and structure ($1-\alpha$). This determines the rate of development into the next stage and the size of store.
- (2) Allocation from store. Females produce eggs from store, whereas diapausing C4s and C5s may use store for structural growth. There is a maximum amount of store available for use per day: $k_1 \cdot x$. We optimise the proportion ε (values between 0 and 1 in steps of 0.1) of the part of stores that are available for use.
- (3) Migration, which determine habitat and thereby activity or diapause. Individuals remain in their present habitat ($\sigma = \text{stay}$) or move to the alternative habitat ($\sigma = \text{migrate}$). Observations suggest that migration between surface and deep waters is an annual routine, which may take considerable time (Atkinson et al. 1997). In the model we simplify this and let animals move between habitats in one day. A vertical migration of more than 1000m has costs, particularly for lipid-rich and positively-buoyant descending individuals (Visser and Jonasdottir 1999, Campbell and Dower 2003). Migration costs are suggested to form a considerable part of the energy budget during overwintering (Jonasdottir 1999). In the model, descending copepods pay a migration cost proportional to total body mass (Table A1).

State dynamics

The three life history decisions influence how structure and store change with time. These state dynamics are presented in Table A2. We assume that net gain of carbon G is converted to structure, store and eggs with the same efficiency (1:1).

Store, however, is an intermediate station and is used for later production of structure or eggs. We assume this to require extra metabolic costs (but see Bonnet, et al. 1998), and use a conversion efficiency $c_{\text{eff}} < 1$. Efficiencies of metabolic pathways are important when evaluating pros and cons of energy storing, but they are not well known; see Saito and Tsuda (2000) for a discussion on conversion from stores to eggs.

Reproduction

When net carbon gain G is positive, fecundity is both food and store dependent. If no carbon is acquired ($G < 0$), fecundity is only store dependent. Fecundity is determined when metabolic costs have been paid. The fecundity (number of female eggs produced per female and day) is then:

$$b(G, y, \epsilon) = \begin{cases} \frac{G + \min(y, k_1 \cdot x) \cdot \epsilon \cdot c_{\text{eff}}}{2 \cdot E} & \text{if } G \geq 0 \\ \frac{\min[(y + G), k_1 \cdot x] \cdot \epsilon \cdot c_{\text{eff}}}{2 \cdot E} & \text{if } G < 0 \end{cases} \quad (\text{A6})$$

Fecundity ($b \geq 0$) is dependent on food and temperature via their effects on G and by the maximum amount of store for use per day $k_1 \cdot x$ ($x = 120$ for all adult females). A sex ratio of 0.5 is assumed, E is egg mass and c_{eff} the conversion efficiency from store to egg.

Table A2. State dynamics of a copepod life history model. Changes in structure x and store y between day t and $t+1$. See Fig. 1 (main text) for carbon flow and Table A1 for parameters.

Habitat	Stage	Dynamics ^a	
		Structure $x_{t+1} =$	Store $y_{t+1} =$
Surface ^b	C4–C5	$x_t + [G \cdot (1 - \alpha)]$	$y_t + [G \cdot \alpha]$
Surface ^b	Adult female ^c	x_t	$y_t - \min[y_t, k_1 \cdot x] \cdot \epsilon$
Deep	C4–C5	$x_t + \min[(y_t + G), k_1 \cdot x] \cdot \epsilon \cdot c_{\text{eff}}$	$y_t + G - \min[(y_t + G), k_1 \cdot x] \cdot \epsilon$
Deep	Adult female	x_t	$y_t + G$

(a) State dynamics are shown when the same habitat is occupied in consecutive time steps. There is a migration cost $c_{\text{mig}} \cdot (x + y)$, drawn from stores, when moving from the surface to the deep habitat. When the habitat z changes from t to $t+1$ the new habitat characteristics (such as metabolism and mortality) influence the copepods from $t+1$.

(b) State dynamics for the surface habitat are shown when net gain $G > 0$.

(c) For simplicity, adult females allocate all net gain to egg production and can not rebuild store. Adult females may, however, have stores if C5s allocate to store before the final moult.

Optimisation algorithm and reproductive value

The optimal allocation of surplus energy $\alpha(x, y, z, t)$, store use $\epsilon(x, y, z, t)$, and habitat choice $\sigma(x, y, z, t)$ (determining activity or diapause) are found for all combinations of structure x , store y , current habitat z , and day of year t using dynamic programming (Houston and McNamara 1999, Clark and Mangel 2000). These actions determine the state-dependent life history strategy, and the optimal strategy is the one maximising reproductive value at each state-time combination.

Maximum reproductive value at time t is found assuming optimal actions for α , ϵ and σ at time t and in the future. Reproductive value must be set at the final time H to start the backward optimization. We set $V(x,y,z,H) = V_{\text{young}}(d,H) = 1$, and iterate the model backwards for several years until the strategies converge and thus become independent of this assumption (Houston and McNamara 1999). With this approach, reproductive value emerges from the model (Houston and McNamara 1999) and represents not only an individual's expected number of female offspring but also the value of the offspring; i.e. the offspring's expected number of own offspring and so on. In this sense it is descendants left far into the future, analogous to the population's long term growth rate, which is optimised. For C4 to adult female, reproductive value V is:

$$V(x, y, z, t) = \max_{\alpha, \epsilon, \sigma} \left\{ P_s(y, z, t) \cdot \left[V(x_{t+1}, y_{t+1}, z_{t+1}, t+1 | \alpha, \epsilon, \sigma) + b(G, y, \epsilon) \cdot V_{\text{young}}(1, t+1) \right] \right\} \quad (\text{A7})$$

Reproductive value V is the sum of future (residual) reproductive value at time $t+1$ and (for adult females) the direct contribution from current egg production (Williams 1966). Both depend on the probability of survival until the next day $P_s(y,z,t)$ as eggs are assumed to be laid at the end of each day. Residual reproductive value depends on the new states obtained, and the state dynamics in turn depend on the actions taken, i.e. α , ϵ , and σ . Current contribution to reproductive value is determined by fecundity b (Eq. A6) and the reproductive value of an egg when reproduction takes place, $V_{\text{young}}(1,t+1)$. The seasonal variation in offspring fitness is an essential property of the model, and it emerges from seasonality in growth, survival, and reproduction opportunities.

Feedbacks from the strategy and back on the environment can not be accounted for with the optimization technique used here. Effects of frequency dependence (including density dependence) on optimal life histories are therefore not tested (Heino et al. 1998). Such questions require other methods such as adaptive dynamics (Dieckmann and Law 1996, Dieckmann and Ferrière 2004) or individual based models (Strand et al. 2002), which tackle less state-dependence and/or are less transparent and tractable.

The state dynamics return values of x and y on the continuous scale, but reproductive value is calculated for discrete values. We use two dimensional linear interpolation for discretization (Mangel and Clark 1988, p. 228), with the exception of continuous values of structure $119 < x < 120$, for which we use the lower integer. The same interpolation is used for abundances in the forward simulation (see below). Forward simulations motivated the exception for the final structure category as it prevents maturation by chance, and instead makes maturation an active decision determined by allocation decisions.

We link the reproductive value of a newly released egg to the reproductive value of a C4 by the use of temperature-, food- and stage-dependent stage transition probabilities, P_{trans} . The reproductive value of a C3 capable of moulting to C4 is linked to the reproductive value of a C4 the next day. Similarly, the previous stages have a reproductive value depending on their probability to develop to the next stage or to remain in the current stage. Reproductive value of a young of stage d is

$$V_{\text{young}}(d, t) = \begin{cases} P_{s\text{Young}}(t) \cdot \left[P_{\text{trans}} \cdot V(15, 5, \text{surface}, t+1) + (1 - P_{\text{trans}}) \cdot V_{\text{young}}(d, t+1) \right] & \text{if } d = 20 \\ P_{s\text{Young}}(t) \cdot \left[P_{\text{trans}} \cdot V_{\text{young}}(d+1, t+1) + (1 - P_{\text{trans}}) \cdot V_{\text{young}}(d, t+1) \right] & \text{if } d \leq 19 \end{cases} \quad (\text{A8})$$

where $P_{s\text{Young}}$ is survival probability and P_{trans} the probability of transition from stage d to $d+1$. Moulting C3s become C4s in the surface habitat with minimum structure ($x = 15 \mu\text{g C}$) and 5% of maximum store ($y = 5$, i.e. $2.25 \mu\text{g C}$).

When plotting reproductive values we first remove the effect of the population growth rate λ (reproductive value is then the same at the end and at the start of the year) and thereafter divide by the egg's seasonal maximum in reproductive value (peak value of an egg is then 1).

Population dynamics

Population dynamics are simulated for females only and we follow the state and stage composition of the population by tracking the proportion of the population occupying any state ($N(x,y,z,t)$ for C4, C5, and adult females) and stage ($N_{\text{young}}(d,t)$ for egg to C3). These proportions are referred to as abundances hereafter. Full scale population simulations are initiated with a set number (optional) of individuals, all with the same state combination ($x = 100, y = 30, z = \text{deep}, t = 1$ (1 July)). We run the forward simulation until the population growth rate λ converges, as it does because the stage- and state-dependent birth and death schedules are constant. For convenience, population size is rescaled to its initial size at the onset of each year, but the new state- and stage-structure is kept. The abundance of young stages (egg to C3) is

$$N_{\text{young}}(d, t + 1) = \begin{cases} \left[\sum_{y=0}^{100} N(120, y, \text{surface}, t) \cdot P_s(y, \text{surface}, t) \cdot b(G, y, \epsilon) \right] + \left[P_{s\text{Young}}(t) \cdot N_{\text{young}}(d, t) \cdot (1 - P_{\text{trans}}) \right] & \text{if } d = 1 \\ P_{s\text{Young}}(t) \cdot \left\{ \left[N_{\text{young}}(d-1, t) \cdot P_{\text{trans}} \right] + \left[N_{\text{young}}(d, t) \cdot (1 - P_{\text{trans}}) \right] \right\} & \text{if } d > 1 \end{cases} \quad (\text{A9})$$

Female eggs enter the population when produced by adult females. The transfer between stages is otherwise a function of survival probability $P_{s\text{Young}}$ and transition probability P_{trans} . The last stage ($d = 20$) has a probability of moulting to C4.

From stage C4 and onwards, the optimal life-history strategy is used in population simulations (Mangel and Clark 1988, p.76–79). We track the abundance of each state category $N(x,y,z,t)$. Discretization of state categories is done by two dimensional linear interpolation as for the estimation of reproductive value (see above). This adds stochasticity to the outcome of state dynamics and results in a spread around the most common state combinations.

Note that separate population simulations, initiated with eggs produced on a given day, are used to study the expected fate of eggs (Fig. 4 and Fig. 6 main text, Fig. A3).

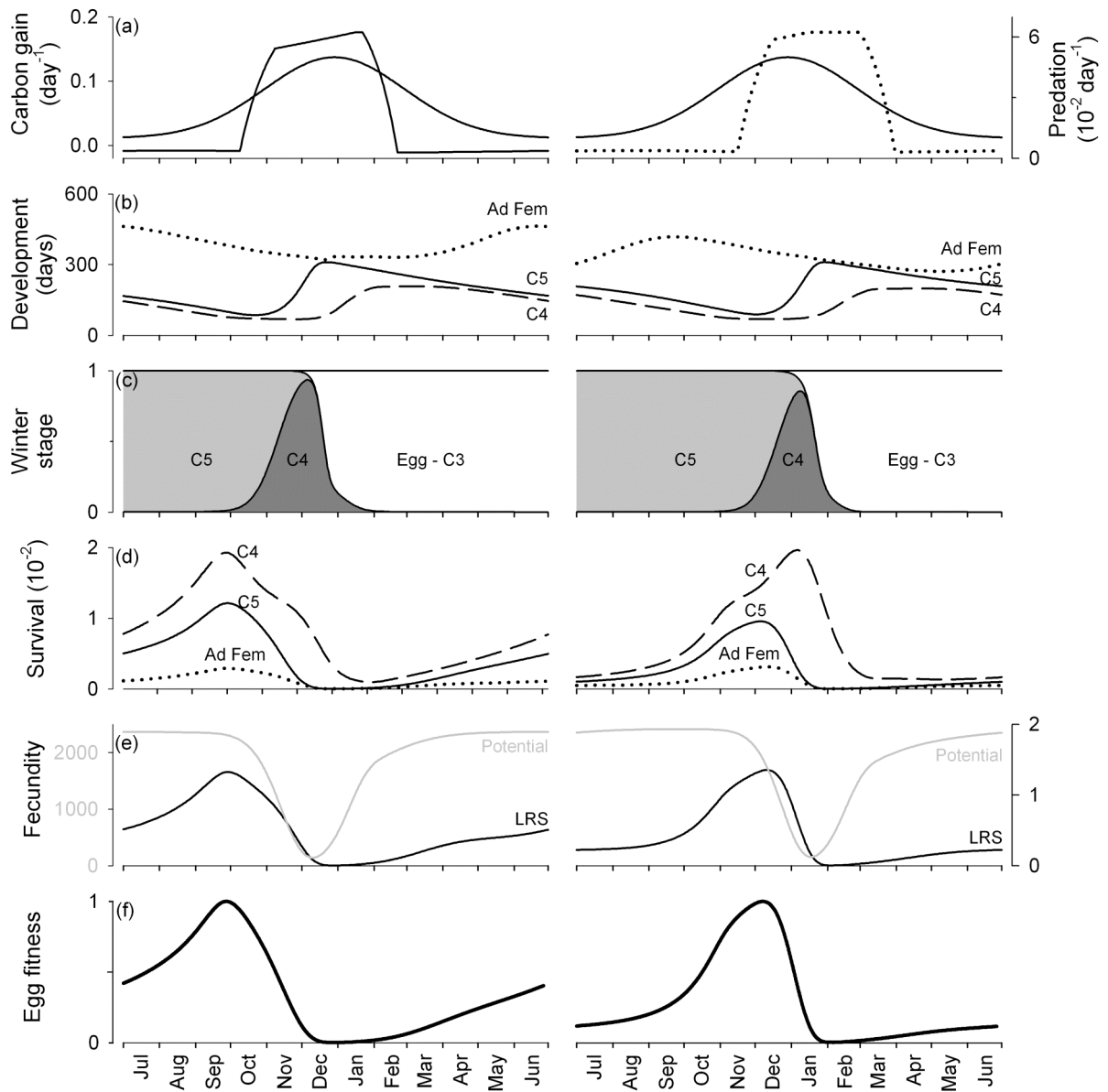


Fig. A3. Expected fate of eggs as predicted from a copepod life history model, with an intermediate (left) and late (right) feeding season. Legend otherwise as for Fig.6 (main text).

References

- Andrews, K. J. H. 1966. The distribution and life-history of *Calanoides acutus* (Giesbrecht). – Discovery Rep. XXXIV: 117–162.
- Atkinson, A. et al. 1997. Regional differences in the life cycle of *Calanoides acutus* (Copepoda: Calanoida) within the Atlantic sector of the Southern Ocean. – Mar. Ecol. Prog. Ser. 150: 99–111.
- Atkinson, A. et al. 1996. Zooplankton response to a phytoplankton bloom near South Georgia, Antarctica. – Mar. Ecol. Prog. Ser. 144: 195–210.
- Bonnet, X. et al. 1998. Capital versus income breeding: an ectothermic perspective. – Oikos 83: 333–342.
- Campbell, R. G. et al. 2001. Growth and development rates of the copepod *Calanus finmarchicus* reared in the laboratory. – Mar. Ecol. Prog. Ser. 221: 161–183.
- Campbell, R. W. and Dower, J. F. 2003. Role of lipids in the maintenance of neutral buoyancy by zooplankton. – Mar. Ecol. Prog. Ser. 263: 93–99.
- Clark, C. W. and Mangel, M. 2000. Dynamic state variable models in ecology. – Oxford Univ. Press.
- Dieckmann, U. and Law, R. 1996. The dynamical theory of coevolution: a derivation from stochastic ecological processes. – J. Math. Biol. 34: 579–612.
- Dieckmann, U. and Ferrière, R. 2004. Adaptive dynamics and evolving biodiversity. – In: Ferrière, R. et al. (eds), Evolutionary conservation biology. Cambridge Univ. Press, pp. 188–224.
- Fiksen, Ø. and Folkvord, A. 1999. Modelling growth and ingestion processes in herring *Clupea harengus* larvae. – Mar. Ecol. Prog. Ser. 184: 273–289.
- Hagen, W. and Schnack-Schiel, S. B. 1996. Seasonal lipid dynamics in dominant Antarctic copepods: energy for overwintering or reproduction? – Deep-Sea Res. Part I 43: 139–158.
- Heino, M. et al. 1998. The enigma of frequency-dependent selection. – Trends Ecol. Evol. 13: 367–370.
- Holm-Hansen, O. et al. 2004. Temporal and spatial distribution of chlorophyll-a in surface waters of the Scotia Sea as determined by both shipboard measurements and satellite data. – Deep-Sea Res. Part II 51: 1323–1331.
- Houston, A. and McNamara, J. 1999. Models of adaptive behaviour. – Cambridge Univ. Press.
- Huntley, M. E. and Lopez, M. D. G. 1992. Temperature-dependent production of marine copepods: a global synthesis. – Am. Nat. 140: 201–242.
- Jonasdottir, S. H. 1999. Lipid content of *Calanus finmarchicus* during overwintering in the Faroe-Shetland Channel. – Fish. Oceanogr. 8: 61–72.
- Mangel, M. and Clark, C. W. 1988. Dynamic modeling in behavioral ecology. – Princeton Univ. Press.
- Michels, J. and Schnack-Schiel, S. B. 2005. Feeding in dominant Antarctic copepods: does the morphology of the mandibular gnathobases relate to diet? – Mar. Biol. 146: 483–495.
- Pasternak, A. F. et al. 1994. Feeding, metabolism and body composition of the dominant Antarctic copepods with comment on their life cycles. – Russ. J. Aquat. Ecol. 3: 49–62.
- Saito, H. and Tsuda, A. 2000. Egg production and early development of the subarctic copepods *Neocalanus cristatus*, *N. plumchrus* and *N. flemingeri*. – Deep-Sea Res. Part I 47: 2141–2158.
- Shreeve, R. S. 2002. Growth of two species of Southern Ocean copepod in relation to their environment. – Open University.
- Shreeve, R. S. and Ward, P. 1998. Moulting and growth of the early stages of two species of Antarctic calanoid copepod in relation to differences in food supply. – Mar. Ecol. Prog. Ser. 175: 109–119.
- Shreeve, R. S. et al. 2002. Copepod growth and development around South Georgia: relationships with temperature, food and krill. – Mar. Ecol. Prog. Ser. 233: 169–183.

- Strand, E. et al. 2002. Artificial evolution of life history and behavior. – *Am. Nat.* 159: 624–644.
- Tarling, G. A. et al. 2004. Life-cycle phenotypic composition and mortality of *Calanoides acutus* (Copepoda: Calanoida) in the Scotia Sea: a modelling approach. – *Mar. Ecol. Prog. Ser.* 272: 165–181.
- Thorpe, S. E. et al. 2004. Tracking passive drifters in a high resolution ocean model: implications for interannual variability of larval krill transport to South Georgia. – *Deep-Sea Res. Part I* 51: 909–920.
- Visser, A. W. and Jonasdottir, S. H. 1999. Lipids, buoyancy and the seasonal vertical migration of *Calanus finmarchicus*. – *Fish. Oceanogr.* 8: 100–106.
- Ward, P. and Shreeve, R. S. 1995. Egg production in three species of Antarctic Calanoid copepods during an austral summer. – *Deep-Sea Res. Part I* 42: 721–735.
- Ward, P. and Shreeve, R. 1998. Egg hatching times of Antarctic copepods. – *Polar Biol.* 19: 142–144.
- Williams, G. C. 1966. Natural selection, the costs of reproduction, and a refinement of Lack's principle. – *Am. Nat.* 100: 687–690.